The use of multispectral digital imagery to map hydrogeomorphic stream units in Soda Butte and Cache Creeks, Montana and Wyoming

by Andrea Wright

A thesis submitted in partial fulfillment of the requirements for the degree of Master of Science in Earth Sciences
Montana State University

Abstract:
Multispectral digital imagery acquired from Soda Butte and Cache Creeks, (Montana and Wyoming) was used in conjunction with field data to classify and map hydrogeomorphic stream units on four stream reaches. Field measurements included water depths, pebble counts, and ground mapping of the hydrogeomorphic units: eddy drop zones, glides, low gradient riffles, high gradient riffles, lateral scour pools, attached bars, detached bars, and large woody debris based on the classification of such units developed by Ladd et ah, 1998. Unsupervised and supervised classification of the imagery was used to develop both a maximum joint probability classification and an alternative joint probability classification of the stream reaches. Classification schemes were developed on the two reaches mapped on Soda Butte Creek and were tested on all other stream reaches in the study after the field maps had been rectified to the imagery. Maximum likelihood classification allowed only one of the image classes to represent each hydrogeomorphic unit on the field map and resulted in relatively low overall accuracies for identification of these units (i.e. 10% to 50%). The 'other likelihood' classification allowed all image classes with a likelihood of occurrence greater than random to represent each hydrogeomorphic unit on the field map (i.e. two or three image classes were assigned to represent each hydrogeomorphic unit) resulting in higher overall accuracies (i.e. 28% to 80%) for identification of these units on the field map. Accurate classification of hydrogeomorphic units was hampered in part by poor rectification of imagery with the field maps due to a lack of ground control points. In general, hydrogeomorphic units largest in area were most likely to be accurately classified while hydrogeomorphic units that were small in area or spatially linear were least likely to be accurately classified. The results of this study demonstrated that multispectral digital imagery has the potential to be a useful tool for mapping hydrogeomorphic stream units at small scales. In order for the imagery to be used as an effective tool, however, careful measures - such as accurate documentation of ground control points, must be taken to ensure accurate rectification of the imagery with field maps.

THE USE OF MULTISPECTRAL DIGITAL IMAGERY TO MAP HYDROGEOMORPHIC STREAM UNITS IN SODA BUTTE AND CACHE CREEKS, MONTANA AND WYOMING

by

Andrea Wright

A thesis submitted in partial fulfillment
of the requirements for the degree

of

Master of Science

in

Earth Sciences

MONTANA STATE UNIVERSITY-BOZEMAN
Bozeman, Montana
April 1998

APPROVAL

of a thesis submitted by

Andrea Wright

This thesis has been read by each member of the thesis committee and has been found to be satisfactory regarding content, English usage, format, citations, bibliographic style, and consistency, and is ready for submission to the College of Graduate Studies

W. Andrew Marcus (Graduate Committee, Chair)	W. Andrew Marcus (Signature)	April 17, 1998 (Date)

Approved for the Department of Earth Sciences

W. Andrew Marcus (Department Head)	W. Andrew Marcus (Signature)	April 17, 1998 (Date)

Approved for the College of Graduate Studies

Joseph Fedock (Interim Graduate Dean)	Joseph J. Fedock (Signature)	4/21/98 (Date)

STATEMENT OF PERMISSION TO USE

In presenting this thesis in partial fulfillment of the requirements for a master's degree at Montana State University-Bozeman, I agree that the Library shall make it available to borrowers under rules of the Library.

If I have indicated my intention to copyright this thesis by including a copyright notice page, copying is allowable only for scholarly purposes, consistent with "fair use" as prescribed in the U.S. Copyright Law. Requests for permission for extended quotation from or reproduction of this thesis in whole or in parts may be granted only by the copyright holder.

Signature Andrea Wright

Date 4/17/98

TABLE OF CONTENTS

LIST OF TABLES

LIST OF FIGURES

ABSTRACT

Multispectral digital imagery acquired from Soda Butte and Cache Creeks, (Montana and Wyoming) was used in conjunction with field data to classify and map hydrogeomorphic stream units on four stream reaches. Field measurements included water depths, pebble counts, and ground mapping of the hydrogeomorphic units: eddy drop zones, glides, low gradient riffles, high gradient riffles, lateral scour pools, attached bars, detached bars, and large woody debris based on the classification of such units developed by Ladd et al., 1998. Unsupervised and supervised classification of the imagery was used to develop both a maximum joint probability classification and an alternative joint probability classification of the stream reaches. Classification schemes were developed on the two reaches mapped on Soda Butte Creek and were tested on all other stream reaches in the study after the field maps had been rectified to the imagery. Maximum likelihood classification allowed only one of the image classes to represent each hydrogeomorphic unit on the field map and resulted in relatively low overall accuracies for identification of these units (i.e. 10% to 50%). The 'other likelihood' classification allowed all image classes with a likelihood of occurrence greater than random to represent each hydrogeomorphic unit on the field map (i.e. two or three image classes were assigned to represent each hydrogeomorphic unit) resulting in higher overall accuracies (i.e. 28% to 80%) for identification of these units on the field map. Accurate classification of hydrogeomorphic units was hampered in part by poor rectification of imagery with the field maps due to a lack of ground control points. In general, hydrogeomorphic units largest in area were most likely to be accurately classified while hydrogeomorphic units that were small in area or spatially linear were least likely to be accurately classified. The results of this study demonstrated that multispectral digital imagery has the potential to be a useful tool for mapping hydrogeomorphic stream units at small scales. In order for the imagery to be used as an *effective* tool, however, careful measures - such as accurate documentation of ground control points, must be taken to ensure accurate rectification of the imagery with field maps.

CHAPTER 1

INTRODUCTION AND PREVIOUS WORK

INTRODUCTION

Reach scale maps of stream channel characteristics are critical for monitoring and understanding changes in channel morphology and documenting riparian and channel habitats for wildlife managers. Data on channel and floodplain characteristics and change have traditionally been collected by research scientists in the field. Historically, most field studies of channel morphology have been based on field surveys at representative, defined river reaches. The drawback to these surveys is that they are local in extent, time consuming, and therefore seldom carried out for more than several years. Aerial photographs have also been used to document channel characteristics since the 1940's and multispectral digital imagery has been used in more recent years. The use of remote sensing has increased because so many of the world's rivers lie in geographically remote areas making field study difficult. Remotely sensed digital imagery also often allows spatial and temporal observation and monitoring of fluvial systems at scales of interest, and provides a data base that is more easily used with computers for quantitative analysis.

The goal of this study is to use digital imagery collected from an airplane and GIS to classify and map hydrogeomorphic stream units in two alpine streams in and adjacent

to Yellowstone National Park. This study will evaluate if variations in spectral reflectances can be used to map channel morphology using a hydrogeomorphic classification system developed by Bisson et al. (1982) and Church and Jones (1982) and modified by Ladd (1995). The distribution of heavy metals following mining were shown to be correlated with these hydrogeomorphic units in Soda Butte Creek, (Ladd, 1995; Marcus et al., 1995a, 1996; Ladd et al., 1998). This study was developed to determine if digital imagery can be used to quickly and effectively map these hydrogeomorphic units on the ground. The objectives of the study are: (1) to field map morphologically distinct stream reaches in the study area, (2) to develop a classification scheme based on the remotely sensed spectral data, and (3) to test the classification algorithms on other mapped stream reaches to determine overall accuracy for use as a mapping tool of this hydrogeomorphic classification scheme.

PREVIOUS WORK

Remotely sensed images, in the form of aerial photography have been used to successfully document changes in fluvial regions since the 1940's (Reeves, 1975). Most studies using aerial photos have focused on documenting changes in the planform of rivers (Lewin and Weir, 1977; Furguson and Werritty, 1983; Ruth, 1988; Schumann, 1989) and variations in water depth (Milton et al., 1995). Studies using aerial photography suffer, however, from the limited extent of coverage of the photos and the frequency with which these photographs are taken.

Satellite imagery has enabled researchers to measure fluvial changes over a larger area of study and on a more frequent basis than air photos (Lyzenga,1980; Ramasamy et al., 1981; Salo and Kalliola, 1986; Jacobberger, 1988; Stumph, 1992; Blasco and Bellan, 1992; Reddy 1993; Mertes et al., 1993). While satellite imagery is useful for measuring and studying small scale fluvial features on large rivers, small scale features that exist at the reach scale on low order streams are better studied with higher resolution, multi-spectral scanner systems attached to airplanes. Gilvear and Watson (1995) used Daedalus Airborne Thematic Mapper data to map floodplains and depth to the water table on streams in Scotland. Daedalus Airborne Thematic Mapper was also used in a similar study (Gilvear and Winterbottom, 1992) to map physical features of a stream reach on the River Tay in Scotland following floods. Hooper (1992) measured spectral response curves from surfaces such as soil, water, and bars in the fluvial environment with this type of multi-spectral imagery.

Two studies that used remotely sensed data to quantify and map morphological channel features are Hardy et al. (1994) and Gilvear et al. (1995). Hardy et al. (1994) classified relative water depths of mesoscale hydraulic features; 'turbulent', 'shoal', 'pool', 'eddy', and 'run', on the Green River, Utah through the use of multi-spectral video imagery. Three band multi-spectral videography in the green (550nm), red (650nm) and near-infrared (850nm) portion of the electromagnetic spectrum was used with spatial resolutions on the order of 0.25 to 3.0 meters. This study found that both unsupervised and supervised classification results showed close agreement between the ground based mapping of these features, although the delineation of water depth was impaired when

turbulence occurred at the surface.

A study in the Circle Mining District of Alaska by Gilvear et al. (1995) used enhanced scanned panchromatic aerial photographs of Faith Creek to provide a quantitative estimate of stream features (runs, glides, and exposed gravel bars) and water depths before and after mining operations on the creek. These photographs varied in scale and the average width of pixels ranged from 13.5m to 17.3m. A logarithmic transformation of the digital number (DN) values was applied to the contrast enhanced aerial photos in an effort to simulate the exponential decline of light levels reaching the substrate with depth. These image processed DN values were compared with known water depths for the stream reach. The highest DN values corresponded with the deep water areas and the lowest DN values corresponded to the shallowest areas of the channel. The results of dividing aerial photographs of the channel from different dates into fifteen water depth categories from the DN values showed that prior to mining in the area, all water depth classes were well represented with many pool-riffle sequences and channel bars. During mining, however, their study found that there was a noticeable absence of deep water areas. These deep water areas increased during the time period following the cessation of mining, although shallow areas still dominated five years later.

Remote sensing has far reaching applications. Remotely sensed data has been successfully used in studies that document channel change, measure vegetation in riparian zones, determine amounts of suspended sediment in ocean environments, map streams, rivers, lakes, and coastlines, model bed planform in rivers, and reconstruct historical river migrations. For the purpose of this study, remotely sensed imagery is supplemented with

field data to create a mapping system for hydraulic-based geomorphologic stream units. Previous studies have successfully used remote sensing to map stream channel morphology, however none to date have attempted to use digital imagery to develop classification methods for mapping the hydrogeomorphic stream units identified in this study. If successful, digital aerial mapping may reduce field costs and help with sampling plans for projects which require knowledge of hydrogeomorphic units (such as metals sampling).

CHAPTER 2

STUDY AREA AND METHODS

STUDY AREA

The two cobble and gravel bed alpine streams selected for this study were Soda Butte Creek and Cache Creek. Four stream reaches were mapped in each stream (a total of eight stream reaches) as part of other ongoing studies. Only two stream reaches of approximately 250 meters in length were selected from each stream (a total of four stream reaches) to be used in this study. The creeks drain adjacent watersheds of similar topography and area (approximately 250 km^2) and flow into the Lamar River inside Yellowstone National Park, Wyoming (Fig. 1).

Both Soda Butte and Cache Creek drain watersheds composed primarily of Eocene volcanic and volcaniclastic rocks (Elliot, 1979). Soda Butte Creek also contains Paleozoic carbonate, shale, and sandstone sediments at its headwaters. Sediments within the stream channels in both watersheds are dominated by cobble and gravel sized particles with occasional pockets of clay and silt.

Soda Butte Creek ranges from an elevation of 3,060m at its headwaters to 2,525m at its confluence with the Lamar River (Table 1). Reach 1, the upper of the two stream reaches in Soda Butte Creek is in a third order braided channel with many small

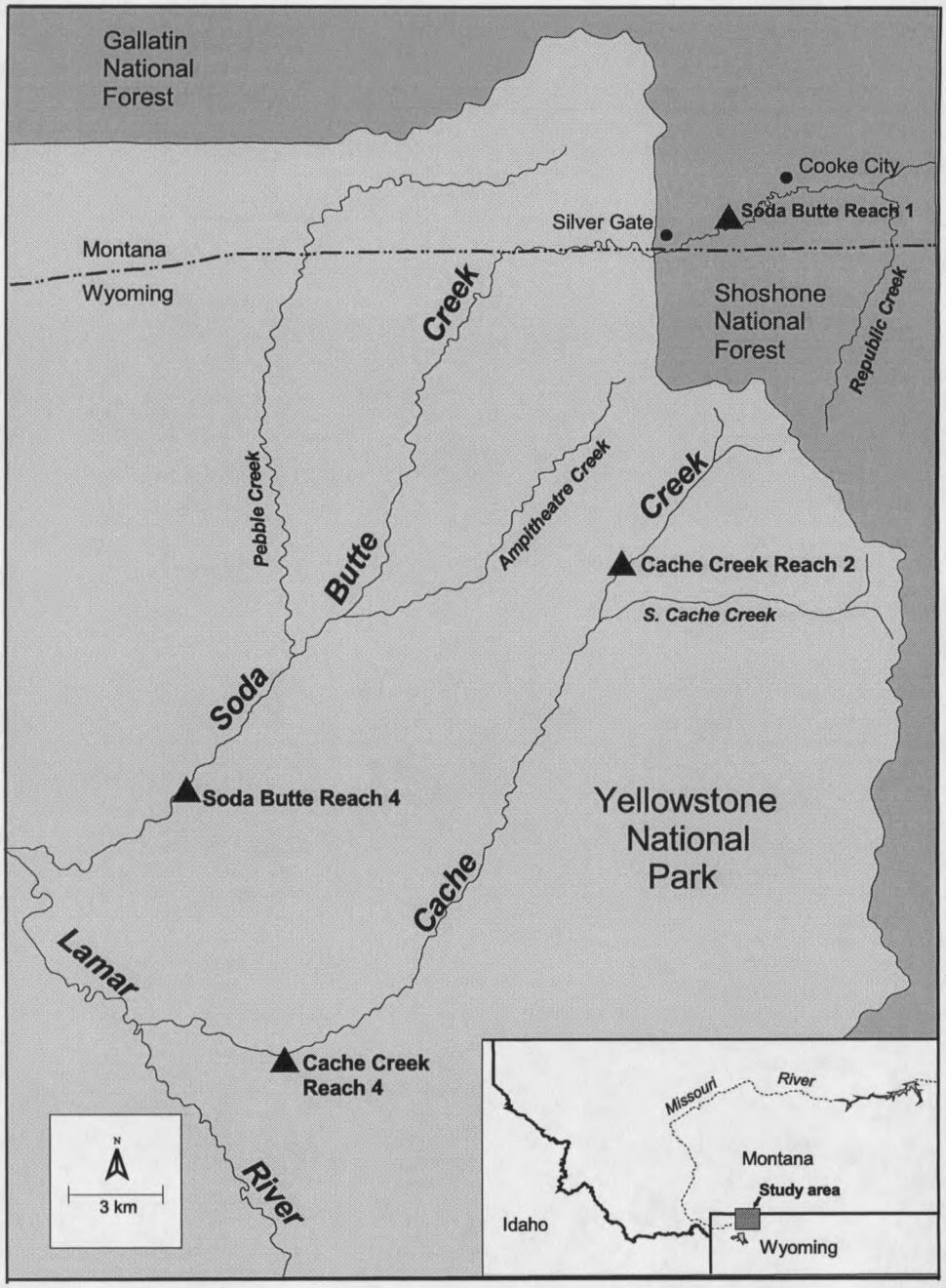

Figure 1 - Study area map of Soda Butte and Cache Creeks

hydrogeomorphologic features (Table 1). Reach 4 is farther downstream and is in a fourth order channel with much larger braided channels and a broad floodplain (Table 1). Soda Butte Creek was largely unaffected by the 1988 Yellowstone fires.

Stream elevations in Cache Creek range from 2,980m at its headwaters to 2,590m at its confluence with the Lamar River (Table 1). Reach 2, the upstream reach, is in a third order channel with relatively small hydrogeomorphic units (Table 1). The downstream reach (Reach 4) is located in a wide fourth order channel and is braided with a broad floodplain (Table 1). The Cache Creek drainage was severely burned by the 1988 Yellowstone fires while the Soda Butte Creek drainage was largely unaffected. These fires have resulted in extensive large woody debris in and along Cache Creek relative to the mapped Soda Butte Creek reaches.

Table 1 - Description of Soda Butte Creek and Cache Creek stream reaches.

Reach #	Length (m)	Maximum Bankfull Width (m)	Average Elevation (m)
Soda Butte 1	252	47	2,900
Soda Butte 4	250	180	2,559
Cache Creek 2	470	43	2,610
Cache Creek 4	280	16	1,925

Vegetation on Soda Butte and Cache Creeks varies with stream reach. Reach 1 in Soda Butte and reach 2 in Cache Creek have vegetation that consists mainly of lodgepole pine and spruce-fir forest. Cache Creek reach 4 and Soda Butte reach 4 are bordered by willow, grasses, forbes, and sedges with occasional lodgepole and cottonwood trees.

METHODS

Field Mapping and Data Collection

Seven types of hydrogeomorphic units were identified and mapped in each of the four study reaches using two systems of classification first proposed by Bisson et. al. (1982) and Church and Jones (1982) and modified by Ladd (1995) for Soda Butte Creek. The modified Bisson et al. classification system was selected because the system was developed for low order forested alpine streams and because it is often used by the U.S. Forest Service and the U.S. Fish and Wildlife Service for stream habitat classification. The Church and Jones system provides a simple classification for emergent bars. The combined classification system used in this study is also being used as part of other ongoing studies in Cache Creek and Soda Butte Creek (Ladd, 1995; Marcus et al., 1996; Ladd et al., 1998). Each of the four study reaches contain seven in-stream hydrogeomorphic units. Attached bars and detached bars were identified following Church and Jones (1982). Glides, lateral scour pools, low gradient riffles, high gradient riffles, and eddy drop zones were identified following Bisson et al. (1982).

Reaches were mapped using 100 m tapes and a Brunton Compass. A 100 m baseline was run along the reach and it's azimuth was determined using a Brunton Compass. Distances to key features were measured along perpendicular transects from the baseline. Global Position Systems (GPS) were used on two different occasions to obtain real world coordinates for the baselines, but in both cases the data was unusable because

of failures at local base stations.

Field mapping of the four stream reaches occurred in the summer months of July and August 1995 after the majority of spring runoff had occurred and the streams were at low flow. This was done to help ensure that no major channel change occurred before the digital data collection commenced in early September 1995.

The hydrogeomorphic units mapped in the four stream reaches varied in size and frequency but were easy to identify visually based on geographic distribution within the stream channel and water surface characteristics (Ladd et al.,1998). Glides have a smooth glassy water surface. They exhibit low turbulence and have a relatively consistent and shallow water depth throughout the unit. Lateral scour pools are identified by both bank and channel bed scour as a result of high velocity flow being diverted along a channel bank. Lateral scour pools often contain the deepest water in the stream and only span a portion of the channel width. Low gradient riffles are identified by having a turbulent flow and generally have the largest surface area of the units in the streams. Low gradient riffles typically span the entire channel width and may be continuous for tens of meters. They appear to have a choppy surface and typically have a bed gradient less than 1%.

High gradient riffles are identified by having turbulent flow and breaking "white" water. Water depth is typically shallow and bed gradients range between 1% and 4%. These units usually contain the largest sized sediments of all the morphological units and are typically dominated by cobbles and gravel. High gradient riffles can be found spanning the entire channel or as isolated units spanning only a portion of the channel.

Eddy drop zones, also called backwater pools, form when an obstruction such as

large woody debris or a bank outcrop diverts flow. These units are identified by a slow eddy current and smooth water surface. Eddy drop zones typically contain the finest sediments of the hydrogeomorphic units.

Attached bars are identified as areas of deposition above water which are connected to the bank on at least one side of the unit. This type of bar typically lacks vegetation and has relatively large sediment size on its surface. Attached bars in the study area tend to be sparsely vegetated, if at all. Detached bars are islands within a stream channel and are areas of deposition. Large detached bars identified in this study were often vegetated with willow and grassses.

Two Wolman pebble counts for two hundred pebbles total (Wolman, 1954) were made for the hydrogeomorphic units in each stream reach on Soda Butte Creek to determine the range of sediment size within each unit. Lateral scour pools were not sampled because depth prohibited collection. Sediment size sampling was done in order to better understand the relationship between morphology and spectral reflectance. One person was responsible for all pebble count measurements to maintain consistency and avoid user bias (Marcus et al., 1995b).

Multispectral digital data from the streams was needed to analyze fine detail on the ground. One meter pixel resolution digital imagery was available locally and was chosen to explore whether standard four band multispectral digital imagery could be used to identify field mapped hydrogeomorphic units. This is important because no existing studies have used this approach. Positive Systems of Kalispell, Montana collected the multispectral data (Table 2) using the raster based digital imaging system ADAR 500

with approximately one meter pixel scale resolution. The time of day of each flight was chosen to minimize shadows from riparian and surrounding vegetation. Flights took place on the 14th of September, 1995 between 11:30am and 1:30pm, when weather had been dry for several days and the water in the streams was clear and sediment free.

Table 2 - Description of spectral bands and band widths used

Band	Bandwidth (nm)	Predominant Color
1	400-480	Blue
2	460-570	Green
3	610-690	Red
4	780-1000	Near Infrared

Image and Data Processing

In order to classify hydrogeomorphic units using multispectral imagery, it was necessary to overlay and register the imagery onto the field maps. To accomplish this, the four field maps of the Soda Butte Creek and Cache Creek stream reaches were digitized as polygons into ARC/INFO (Figs. 2 and 3). Water depths, sediment size, and vegetation attributes were then assigned to each individual hydrogeomorphic unit from data collected in the field. The digitized field maps were converted into raster maps in the ARC/INFO module GRID, with a 1m cell size. The multispectral images were georectified to the raster field maps of each corresponding reach using ERDAS Imagine, so the two data sets could be overlaid. Lack of precision in the ground truth maps, due in part to failure of GPS control, created significant problems with georectification. These

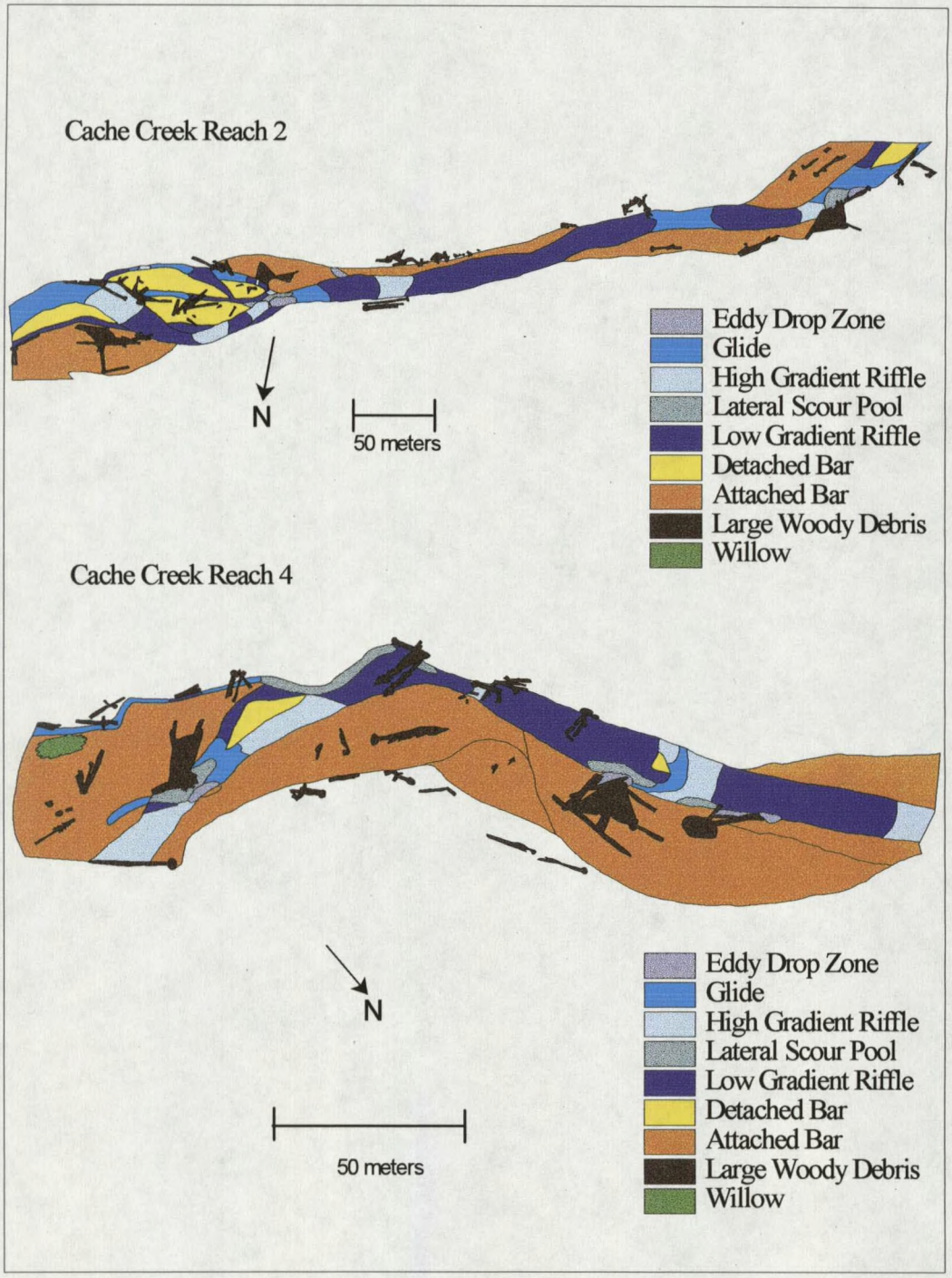

Figure 2 - Hydrogeomorphic units of Cache Creek Reaches 2 and 4

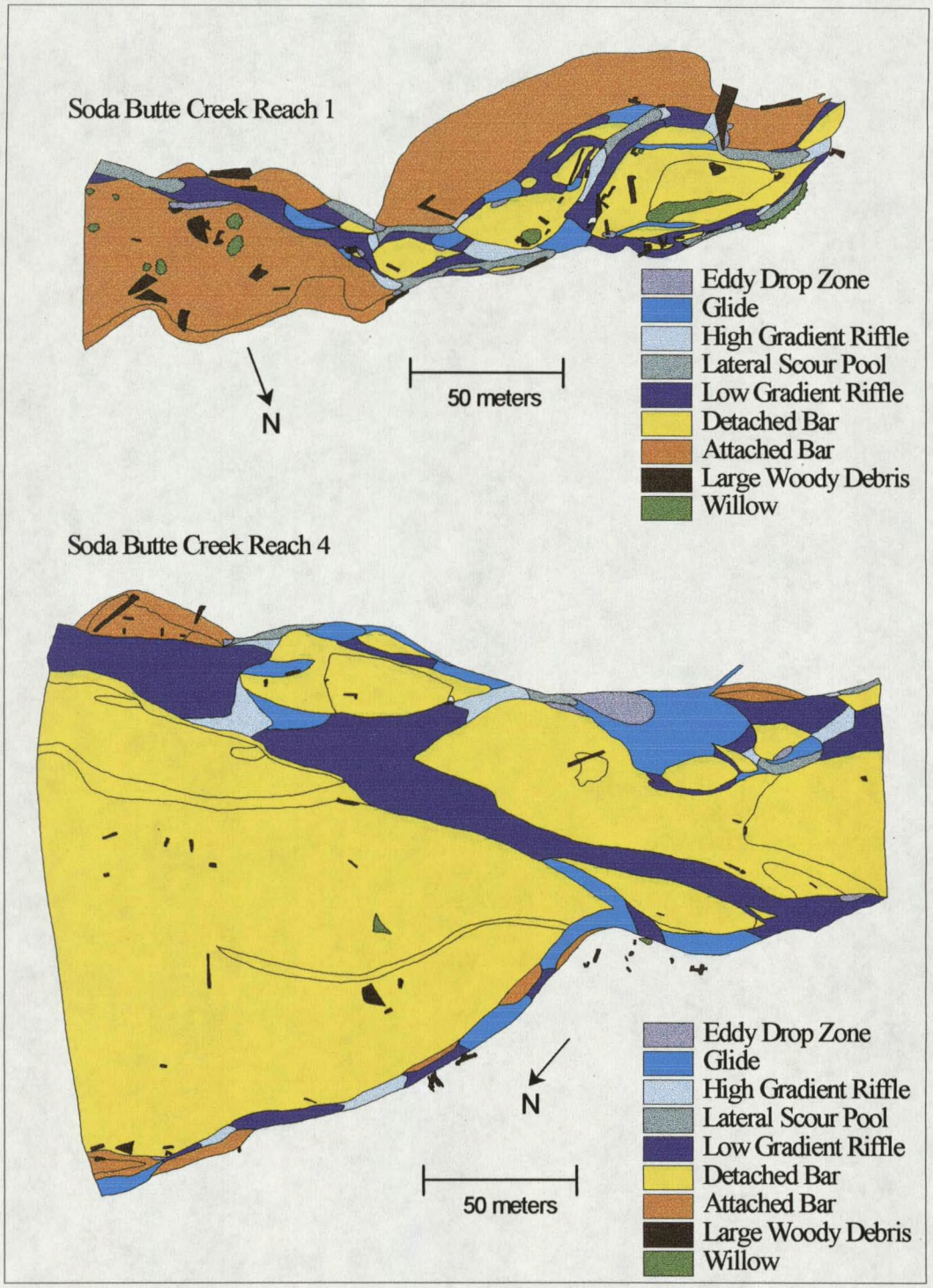

Figure 3 - Hydrogeomorphic units of Soda Butte Creek Reaches 1 and 4

problems will be discussed in Chapter 4.

No enhancement procedures were used with the multispectral digital imagery because of known error introduced into the study during the rectification process. Enhancement of the imagery would not improve classification results. Furthermore, altering the data would make the methodology less readily transferrable to future studies.

Classification

Standard supervised classification schemes such as minimum distance approaches (Swain and Davis, 1978 as cited in Erdas, Inc., 1997 and Sabins, 1987) could not be used because of problems with georectification. The difficulties were compounded because many of the hydrogeomorphic units were only a meter or two in width (Figs. 2 and 3). Georectification errors of only one or two meters therefore led to inaccurate overlays of field mapped units and spectral imagery. In traditional supervised classification techniques, a spectral signature is created by selecting multiple pixels that define a category (or map unit) on the ground from the imagery. Because many of the map units in this study were represented by 2 or fewer pixels on the imagery, standard supervised classification approaches were not practical.

A new method for classification of multispectral digital imagery was developed based on the work of Aspinall (1992) and Fisher (1989). The method is based on the probabilities that the image classes predict the field mapped units on the ground and that the field mapped units predict the imagery. Figure 4 is a simplified example of an image

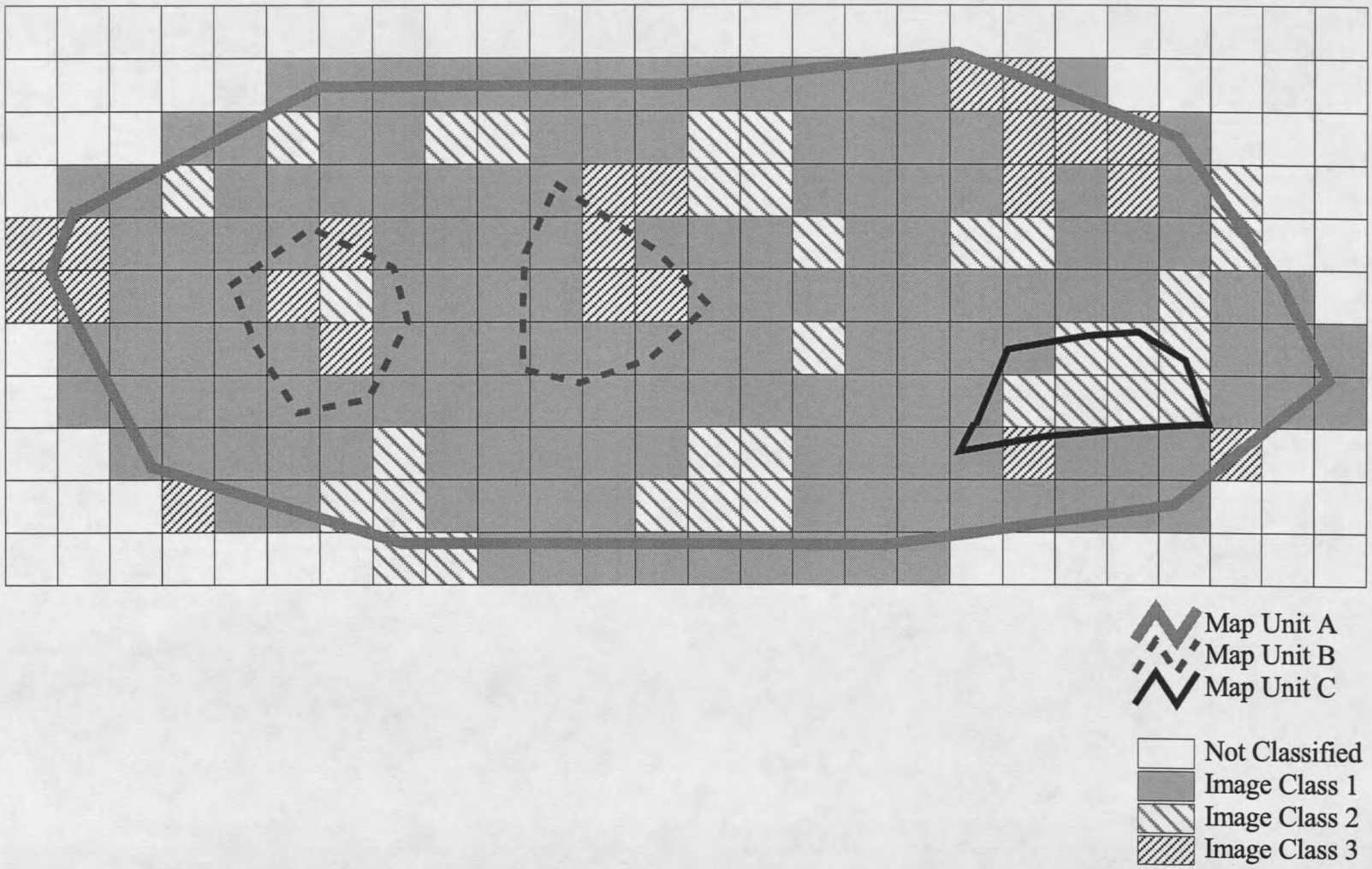

Figure 4- Simplified example of map and image overlay.

and field map that helps clarify the procedure used in this study.

First, an unsupervised classification of the imagery is performed. The example image (Fig. 4) has been classified into three image classes; Image Class 1, 2, and 3. These three unsupervised image classes then are overlaid onto a field map composed of three map units: A, B, and C (Fig. 4). To evaluate the relationship of the three image classes to the three map units, two factors were considered: 1) how image classes are represented on the ground, and 2) how map units on the ground are represented by the imagery. To do this, a technique of evaluating Image Class Probability and Map Unit Probability was developed.

Image Class Probability is the probability that each image class can represent each map unit (Table 3, Fig. 4). The pixels in Figure 4 that are in Image Class 1 are scattered across the map (Fig. 4). To calculate Image Class Probability for each map unit, a count is made of all pixels in Image Class 1 that fall into Map Unit A, all of the pixels in Image Class 1 that fall into Map Unit B, and all of the pixels in Image Class 1 that fall into Map Unit C (fractional pixels are summed and a whole pixel is counted as one). Each of these counts is then divided by the total number of pixels in Image Class 1 and multiplied by 100 to get the percent probability that Image Class 1 can represent each of the 3 map units (Table 3).

Table 3 - Example derivation of Image Class Probability

	# of Image Class 1 pixels	# Image Class 1 pixels in Map Unit / total # pixels in Image Class 1	Image Class % Probability
Map Unit A	146	0.94	94%
Map Unit B	8	0.05	5%
Map Unit C	1	0.01	1%
total # pixels	155		

Next, the percent probabilities that Image Class 2 represents each map unit in Figure 4 and that Image Class 3 represents each map unit in Figure 4 are calculated in the same way. A three by three matrix is generated of map units by Image Class Probabilities (Table 4). Each element in the matrix (Table 4) is an Image Class Probability.

Table 4 - Example Image Class Probabilities derived from data in Figure 4.

	Map Unit A	Map Unit B	Map Unit C
Image Class 1	94%	5%	1%
Image Class 2	76%	3%	21%
Image Class 3	71%	29%	0%

Once the probabilities that the image classes predicted the map units has been calculated in the form of Image Class Probabilities (Table 3), the probabilities that the Map Units predict the imagery are determined. This is the Map Unit Probability, or the probability that each map unit on the ground represents each of the image classes. Here each of the map units in Figure 4 is examined separately, beginning with Map Unit C. Within the boundary of Map Unit C there are pixels from each of the three image classes.

First count the number of pixels in Map Unit C that belong to Image Class 1, Image Class 2, and Image Class 3. Next, divide each of these counts by the total number of pixels that comprise Map Unit C and then multiply by 100 to get the Map Unit Probability (Table 5).

Table 5 - Example derivation of MapUnit Probability

	# of pixels in Map Unit C	# Map Unit C pixels in Image Class / total # pixels in Map Unit C	Map Unit % Probability
Image Class 1	1	0.14	14%
Image Class 2	6	0.86	86%
Image Class 3	0	0.00	0%
Total in C	7		

Next the percent probabilities that Map Unit B represents each image class in Figure 4 and that Map Unit A represents each image class in Figure 4 are calculated in the same way. The results of these calculations can be put into a 3 by 3 matrix of Map Unit Probability by image class (Table 6).

Table 6 - Example Map Unit Probabilities derived from Figure 4.

	Map Unit A	Map Unit B	Map Unit C
Image Class 1	75%	53%	14%
Image Class 2	14%	7%	86%
Image Class 3	11%	40%	0%

The next step is to determine the relationship between Image Class and Map Unit Probabilities. This is done by calculating a joint probability index using the equation:

$$\frac{[(MUP)\ (ICP)]}{[(100\ -\ ICP)\ (100\ -\ MUP)\ +\ (MUP)\ (ICP)]} \qquad (1)$$

where MUP is the map unit percent probability and ICP is the image class percent probability described above (Aspinall, 1995).

This joint probability index is a relative measure of agreement between Map Unit and Image Class Probabilities. Using equation 1, a 3 by 3 matrix of joint probability indices can be generated using the values from Tables 4 and 6 (Table 7). The higher the index value, the higher the agreement between these two probabilities, and therefore the higher the likelihood that the map unit will be predicted by the image class and vice versa.

Table 7 - Example joint probability indices.

	Map Unit A	Map Unit B	Map Unit C
Image Class 1	0.979	0.051	0.002
Image Class 2	0.340	0.002	0.620
Image Class 3	0.232	0.210	0.000

Once the joint probability indices are calculated, the classification schemes are analyzed using two methods. The first method, the Maximum Joint Probability method, uses the highest joint probability index to classify the data. This method examines the rows of the joint probability index matrix (Table 7) and selects the highest map unit index value to represent that image class. The highest index value for Image Class 1 corresponds to the index value for Map Unit A (0.979), the highest index value for Image

Class 2 corresponds to the index value for Map Unit C (0.620), and the highest index value for Image Class 3 corresponds to the index value for Map Unit A (0.232), (Table 7).

The Maximum Joint Probability classification scheme assigns pixels in the image classes to map units based on their highest joint probability index value. Supervised classifications can now be performed on other mapped areas using the three image classes and evaluated for accuracy. All pixels in Image Class 1 that fall into Map Unit A are deemed correctly classified, all pixels in Image Class 2 that fall into Map Class C are deemed correctly classified, and all pixels in Image Class 3 that fall into Map Class A are deemed correctly classified. Any pixels in these Image Classes that do not fall into the representative Map Unit are deemed incorrectly classified. Note that Map Unit B did not contain the highest joint probability index value in any of the three Image Classes in this example. Therefore, no pixels will be classified as Map Unit B in further supervised classifications. The Maximum Joint Probability method of classification allows each image class to represent only one map unit.

An alternative classification system is needed if Map Unit B is to be recognized in the image classes. This new method of classification is called the Alternative Joint Probability method of classification. This method examines all map unit index probabilities in each image class that have a value greater than random (are over-represented). To determine which map units meet this criteria, the random joint probability index must be evaluated with equation 1. Although 'random' joint probability can be calculated by weighting for different factors such as area, this method assumes no relationship between map units and image classes and no weighting procedures are used. Using the example in

Figure 4, there are 3 map units and 3 image classes. Therefore the probability of any randomly located pixel falling into any image class is 1 in 3 (or 33%) and the probability of any randomly located pixel falling into a given map unit is also 1 in 3 (or 33%). By using these values in equation 1 a random joint index probability of 0.20 is calculated for this example (equation 1). All Map Units that have a joint probability index value greater than 0.20 in any Image Class in Table 7 are therefore included in this analysis. Table 8 illustrates all joint probability index values that were included in the Alternative Joint Probability analysis in this example.

Table 8 - Example of Alternative Joint Probability Method. All index values included in this analysis are highlighted in gray. All other values are lower than the random joint probability value of 0.20.

	Map Unit A	Map Unit B	Map Unit C
Image Class 1	0.979	0.051	0.002
Image Class 2	0.340	0.002	0.620
Image Class 3	0.232	0.210	0.000

The highlighted values in rows of Table 8 can now be used as a basis for classification. For Image Class 1, only pixels in Map Unit A are considered correctly classified. For Image Class 2, pixels that fall into Map Unit A and pixels that fall into Map Unit C are considered correctly classified. For Image Class 3, pixels that fall into Map Unit A and pixels that fall into Map Unit B are considered correctly classified. So, Image Classes 1 and 3 can now be allowed to represent two map units on the ground as compared to just one map unit as in the Maximum Joint Probability method and Map

Unit B is now recognized in this classification. This type of analysis allows the series of Image Class and Map Unit indices to provide a form of fuzzy classification (Fisher, 1989), where some map units are defined by multiple image classes, and some by only one.

These methods were applied to the data collected from Soda Butte and Cache Creeks. Classifications were developed following the steps outlined above on Soda Butte reach 1 and Soda Butte reach 4. The imagery was divided into 30 classes and overlain onto the field maps which had 8 units. These classifications were then tested on the development reaches to determine initial accuracy and then on the three other stream reaches in the study area.

The accuracy of these classification schemes was assessed by creating a confusion matrix (Aspinall and Pearson, 1995). A confusion matrix is a table that compares classes identified on the field map with classes identified on the classified imagery. From the rows and columns of a confusion matrix, errors of commission and omission (user's and producer's accuracy respectively) as well as percent correctly classified can be derived for the entire map, and for individual map units. Confusion matrices can also be used to determine which map units are confused with each other, or are incorrectly classified as well as to identify Alternative Joint Probability classes . The results of analysis from confusion matrices is discussed in Chapter 4.

CHAPTER 3

DATA

Several types of data were collected to explore the reasons for different spectral signatures of the hydrogeomorphic units (Fig. 2 and 3). Differences in sediment size among hydrogeomorphic units were derived from Wolman pebble counts on Soda Butte Creek (Table 9). Two hundred pebbles were counted in riffles, glides, and eddy drop zones. Eddy drop zones are the only hydrogeomorphic unit with a significantly distinct distribution of sediment size (Table 9). Water depths were measured for each of the hydrogeomorphic units in each reach where appropriate, and the range and mean in water depth for each type of unit was calculated (Table 10). Lateral scour pools tend to be the deepest of the hydrogeomorphic units, and riffles the shallowest (Table 10). Variability among stream reaches is also evident in the range of pixel values (which run from 0 to 255) gathered from the raw digital data (Table 11). Cache Creek does not have the lower digital numbers in all bands that exist in the Soda Butte Creek data (Table 11). The frequency and area of hydrogeomorphic units, and the proportion of the total reach each type of hydrogeomorphic unit comprised are shown in Table 12. Overall, bars and low gradient riffles are have the highest frequency and cover the most area in the stream reaches, while eddy drop zones and lateral scour pools have the lowest frequencies and cover the least amount of area (Table 12).

Table 9 - Percentile distribution of sediment size (mm) in Soda Butte Creek by hydrogeomorphic unit.

	Soda Butte Reach 1						Soda Butte Reach 4					
	HGR	LGR	G	EDZ	AB	DB	HGR	LGR	G	EDZ	AB	DB
D_{10}	30	23	20	2	26	31	42	50	27	2	40	33
D_{50}	66	71	44	2	72	70	80	90	74	2	84	76
D_{90}	123	116	93	15	120	122	126	146	130	12	133	124

HGR = high gradient riffle, LGR = low gradient riffle, G = glide, EDZ = eddy drop zone, AB = attached bar, DB = detached bar.

Table 10 - Range of water depths of hydrogeomorphic units in Soda Butte and Cache Creeks.

	Soda Butte 1		Soda Butte 4		Cache Creek 2		Cache Creek 4	
	Range (cm)	Mean (cm)	Range (cm)	Mean (cm)	Range (cm)	Mean (cm)	Range (cm)	Mean (cm)
Glide	3-46	16.8	7-60	25.3	5-40	22.7	3-46	18.5
Lateral Scour Pool	16-44	31.8	27-60	42.3	30-150	90.0	24-100	58.0
Low Gradient Riffle	2-22	13.0	5-60	21.5	5-33	16.3	8-37	19.8
High Gradient Riffle	10-30	16.1	7-70	25.7	5-28	16.1	10-30	22.5
Eddy Drop Zone	5-40	16.8	15-80	33.2	5-32	15.5	17-63	30.0

Table 11 - Range in pixel values (digital number) by band for each reach.

	Soda Butte 1		Soda Butte 4		Cache Creek 2		Cache Creek 4	
	range	mean	range	mean	range	mean	range	mean
Band 1	32-134	64.7	32-148	73.9	42-117	66.2	41-125	70.2
Band 2	41-255	129.3	46-255	141.9	52-252	122.9	43-255	124.1
Band 3	28-255	109.6	34-255	134.2	46-255	111.4	45-255	118.2
Band 4	34-251	110.1	35-255	149.9	34-252	99.1	38-255	114.2

Table 12 - Description of the range and mean area (m^2), frequency (n), and percent area of hydrogeomorphic units in Soda Butte Creek and Cache Creek stream reaches.

	Soda Butte 1				Soda Butte 4				Cache Creek 2				Cache Creek 4			
	Range (m^2)	Mean (m^2)	n	% Area	Range (m^2)	Mean (m^2)	n	% Area	Range (m^2)	Mean (m^2)	n	% Area	Range (m^2)	Mean (m^2)	n	% Area
EDZ	1-39	9	13	0.9	3-181	40	6	1.0	14-56	31	4	1.0	14-25	19	4	0.7
G	8-103	47	9	3.5	17-804	167	12	8.0	1-518	158	10	12.8	2-114	37	9	2.9
LSP	22-123	78	8	5.2	23-65	46	4	0.7	35-94	65	2	1.1	13-130	63	5	2.8
LGR	17-383	110	16	12.0	15-2599	364	13	18.7	1-1572	233	15	28.4	9-690	248	7	15.2
HGR	1-90	26	11	2.4	5-177	66	8	2.1	5-346	109	8	7.0	1-253	114	7	6.9
DB	1-456	100	18	19.1	6-14134	1074	22	65.2	0.3-497	205	8	1.4	8-216	79	2	1.4
AB	48-2784	1082	6	53.7	0.4-1077	90	11	3.9	0.4-1077	458	10	37.7	4-21367	704	10	61.4
LWD	2-74	16	25	3.3	1-28	11	12	0.5	2-233	57	23	10.7	2-273	32	32	8.8

EDZ = Eddy Drop Zone, G = Glide, LSP = Lateral Scour Pool, LGR = Low Gradient Riffle, HGR = High Gradient Riffle, DB = Detached Bar, AB = Attached Bar, LWD = Large Woody Debris.

CHAPTER 4

ANALYSIS AND DISCUSSION

SPECTRAL DATA

The two classifications developed on Soda Butte Creek reaches 1 and 4 resulted in slightly different spectral classes for the seven hydrogeomorphic units. The mean plots for the spectral signatures of each type of hydrogeomorphic unit are shown in Figures 5 and 6. Note that no successful classification for eddy drop zones was developed from the Soda Butte reach 1 development site or for high gradient riffles from the Soda Butte reach 4 development site (Figs. 5 and 6). This result is discussed further in this chapter.

MAXIMUM JOINT PROBABILITY CLASSIFICATION

The Maximum Joint Probability results of the two classifications developed on Soda Butte reach 1 and Soda Butte reach 4 are shown in Table 13. Each classification was tested on the site from which it was developed to determine initial development accuracy. The accuracy of the classification based on the Soda Butte reach 4 development site was 16% higher overall than that of the Soda Butte reach 1 development site. In contrast, the classification developed on Soda Butte reach 1 had a higher percent correctly

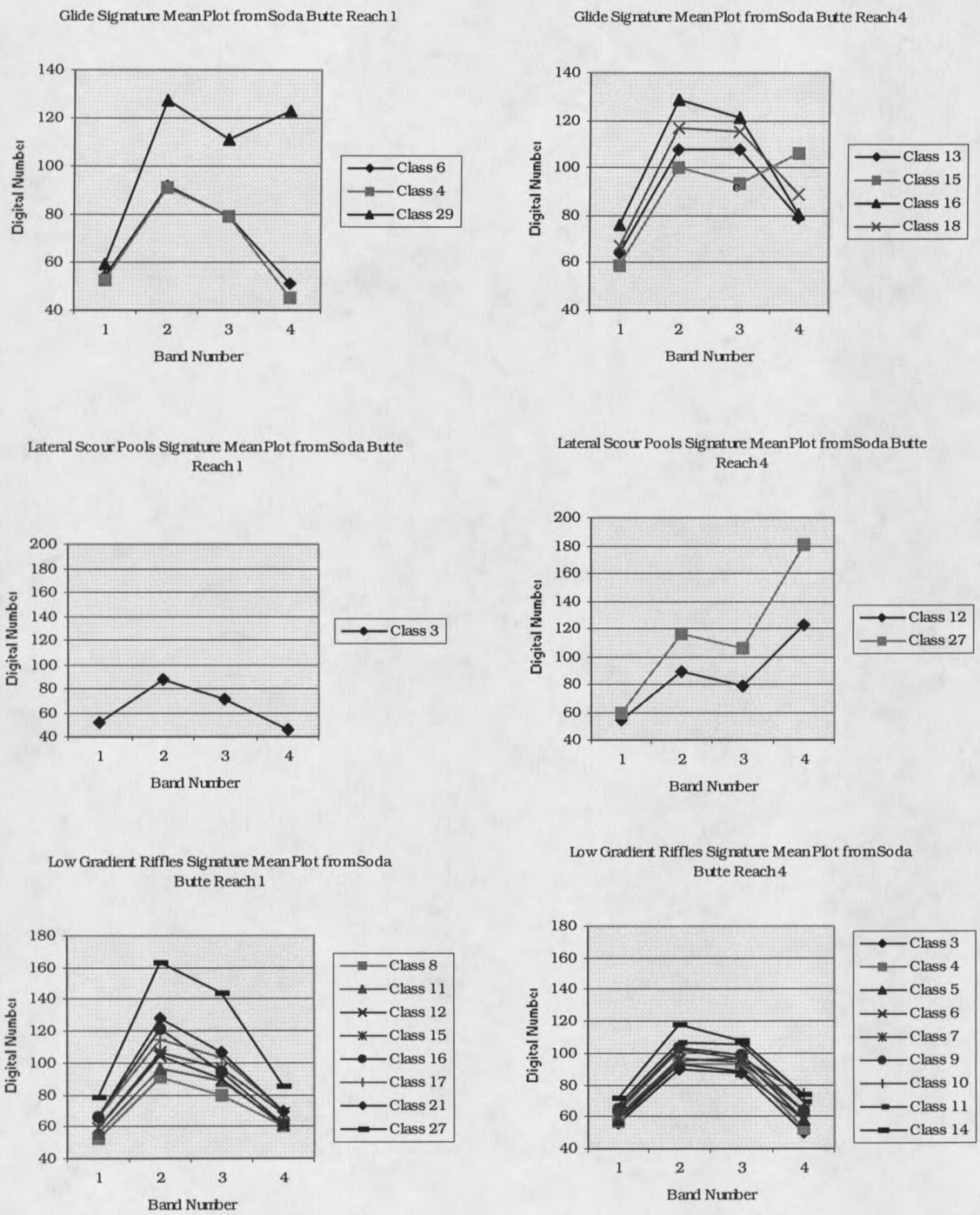

Figure 5 - Signature mean plots derived from Soda Butte Creek reach 1 and reach 4 for glides, lateral scour pools, and low gradient riffles.

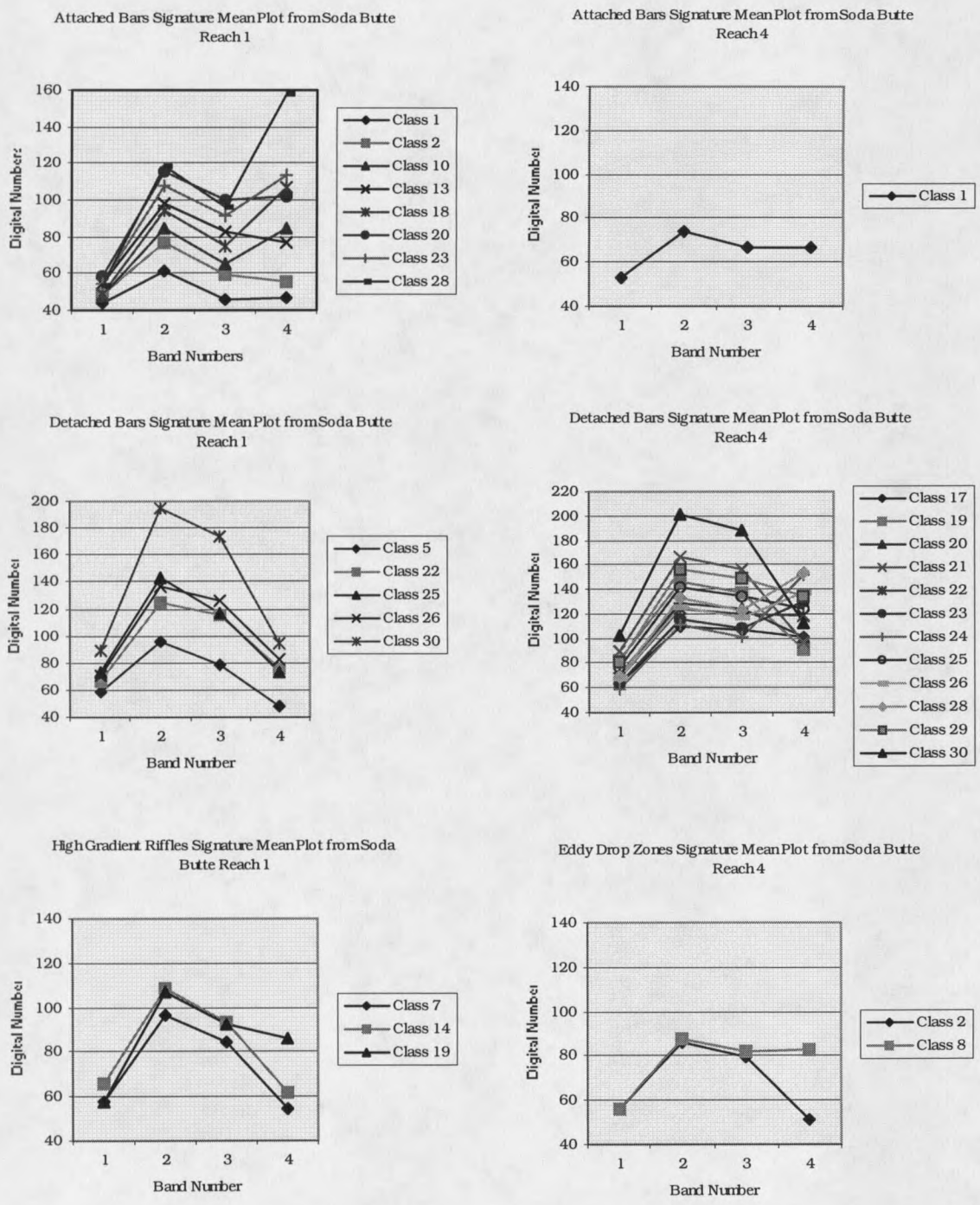

Figure 6 - Signature mean plots derived from Soda Butte Creek reach 1 and reach 4 for attached bars, detached bars, high gradient riffles, and eddy drop zones.

classified on the Cache Creek reaches than did the classification based on Soda Butte 4.

Table 13 - Percent of hydrogeomorphic units correctly classified for each stream reach using the Maximum Joint Probability classification.

Development Site	Test Site	Percent Correctly Classified
Soda Butte 1	Soda Butte 1	37.7%
Soda Butte 1	Soda Butte 4	35.2%
Soda Butte 1	Cache Creek 2	21.2%
Soda Butte 1	Cache Creek 4	16.7%
Soda Butte 4	Soda Butte 4	53.2%
Soda Butte 4	Soda Butte 1	23.7%
Soda Butte 4	Cache Creek 2	18.8%
Soda Butte 4	Cache Creek 4	10.5%

The results in Table 13 were derived from confusion matrices generated from each of the test sites, an example of which is shown in Table 14. Overall percent correctly classified was calculated for each stream reach in the study by dividing the row total of each confusion matrix by the diagonal column totals as highlighted in Table 14 and then multiplying this proportion by 100 (Lillesand and Keifer, 1994). Numerical row and column values in the matrix are absolute pixel counts. Confusion matrices derived from test results of all other stream reaches tested are in Appendix A.

The accuracy of class identification for each hydrogeomorphic unit or map unit can be evaluated by examining confusion matrices of commission, also known as users accuracy and confusion matrices of omission, also known as producer's accuracy. Confusion matrices of commission indicate the probability that pixels on the imagery

Table 14 - Confusion matrix for Soda Butte reach 1 development site tested on Soda Butte Reach 1. Values in the matrix represent number of pixels.

Confusion Matrix - Soda Butte Reach 1 Development Site[1]									
		Field Map							
		EDZ	G	LSP	LGR	HGR	DB	AB	LWD	Row Total
Classified Imagery	EDZ	**0**	0	0	0	0	0	0	0	0
	G	2	**125**	38	133	14	35	9	3	359
	LSP	2	18	**20**	21	10	24	2	0	97
	LGR	17	95	164	**595**	64	271	68	30	1303
	HGR	11	42	49	144	**83**	60	19	15	423
	DB	15	50	69	157	56	**193**	40	23	603
	AB	5	24	43	139	5	13	**225**	40	495
	LWD	0	1	3	11	9	4	11	**14**	53
Column Total		52	355	386	1200	241	600	374	125	3333
Percent Correctly Classified 37.65 %										

[1]EDZ = eddy drop zone, G = glide, LSP = lateral scour pool, LGR = low gradient riffle, HGR = high gradient riffle, DB = detached bar, AB = attached bar, LWD = large woody debris

classified into a given category (or map unit) actually represent that category on the ground (Sabins, 1987).

These user's accuracies are found by dividing the number of correctly classified pixels in each class by the total number of pixels classified in that class. Confusion matrices of omission indicate how well pixels in the imagery are classified (Sabins, 1987). These producer's accuracies are found by dividing the number of correctly classified pixels in each category by the number of pixels in that category. It is important to examine the overall percent correctly classified *and* the percent correctly classified of each individual type of hydrogeomorphic unit in each stream reach to better understand when and why the classification schemes accurately depict the field mapped data.

An example of a confusion matrices for commission and omission is shown for the Soda Butte reach 1 development site in Table 15 (these matrices for all other stream reaches are shown in Appendix B). In the commission matrix, row values are normalized

Table 15 - Confusion matrices of commission and omission for Soda Butte reach 1 development site tested on Soda Butte reach 1

Error of Commission - Soda Butte Reach 1[1]									
User's Accuracy		Field Data							
		EDZ	G	LSP	LGR	HGR	DB	AB	LWD
Classified Imagery	EDZ	**0.00**	0.00	0.00	0.00	0.00	0.00	0.00	0.00
	G	0.56	**34.82**	10.58	37.05	3.90	9.75	2.51	0.84
	LSP	2.06	18.562	**20.62**	21.65	10.31	24.74	2.06	0.00
	LGR	1.30	7.29	12.58	**45.63**	4.91	20.78	5.21	2.30
	HGR	2.60	9.93	11.58	34.04	**19.62**	14.18	4.49	3.55
	DB	2.49	8.29	11.44	26.04	9.29	**32.01**	6.63	3.81
	AB	1.01	4.86	8.70	28.14	1.01	2.63	**45.55**	8.10
	LWD	0.00	1.89	5.66	20.75	16.98	7.55	20.75	**26.42**

Error of Omission - Soda Butte Reach 1									
Producer's Accuracy		Field Data							
		EDZ	G	LSP	LGR	HGR	DB	AB	LWD
Classified Imagery	EDZ	**0.00**	0.00	0.00	0.00	0.00	0.00	0.00	0.00
	G	3.85	**35.21**	9.84	11.08	5.81	5.83	2.41	2.40
	LSP	3.85	5.07	**5.18**	1.75	4.51	4.00	0.53	0.00
	LGR	32.69	26.76	42.49	**49.58**	26.56	45.17	18.18	24.00
	HGR	21.15	11.83	12.69	12.00	**34.44**	10.00	5.08	12.00
	DB	28.85	14.08	17.88	13.08	23.24	**32.17**	10.70	18.40
	AB	9.62	6.76	11.14	11.58	2.07	2.17	**60.16**	32.00
	LWD	0.00	0.28	0.78	0.92	3.73	0.67	2.94	**11.20**

[1] See Table 14 for hydrogeomorphic unit abbreviations.

percents. Column values are normalized percents in the omission matrix. Highlighted diagonal column values are the percent correctly classified for each type of hydrogeomorphic unit in the study sites given users (commission) and producers (omission) accuracies. The percent correctly classified for each hydrogeomorphic stream unit in each stream reach derived from confusion matrices of user's and producer's accuracies are summarized in Tables 16 and 17 respectively.

Confusion matrices of these types can be used to determine which classes are confused, or incorrectly classified as well as to identify alternative joint probability classes to accompany the maximum joint probability class. For all of the study sites, eddy drop zones, lateral scour pools, and high gradient riffles were most often misclassified. Glides, low gradient riffles, and detached bars were most often correctly classified. Further evaluation and explanation of these results will be discussed later in this chapter.

The best overall results of the Maximum Joint Probability classification are found on the development sites when tested on themselves (Table 13), but these classifications do not transfer as well to other areas. Tests on the Soda Butte stream reaches yielded a relatively higher percent correctly classified than tests on the Cache Creek reaches. This may be a result of morphologic differences that exist between the two streams. Overall, the Cache Creek reaches have more large woody debris present, lack well developed braiding systems, and exhibit a higher proportion of attached bars and lower proportion of detached bars than do the Soda Butte stream reaches (Figs. 2 and 3).

Table 16 - Percent correctly classified of each hydrogeomorphic unit in the Soda Butte and Cache Creek development and test sites as derived from user's accuracies using the Maximum Joint Probability classification.

Hydrogeomorphic Units									
Study Sites		Eddy Drop Zone	Glide	Lateral Scour Pool	Low Gradient Riffle	High Gradient Riffle	Detached Bar	Attached Bar	Large Woody Debris
Development[1]	Test[1]								
SB1	SB1	0.0	34.8	20.6	45.6	19.6	32.0	45.6	26.4
SB1	SB4	0.0	11.9	16.0	57.4	4.8	34.6	18.7	0.6
SB1	CC2	0.0	7.3	4.1	36.8	13.3	10.8	28.3	18.7
SB1	CC4	0.0	3.5	5.7	38.6	14.4	6.0	11.4	26.9
SB4	SB4	14.2	30.5	12.2	66.0	0.0	50.7	50.9	0.0
SB4	SB1	0.3	5.4	3.7	40.2	0.0	25.1	33.6	0.0
SB4	CC2	2.7	8.4	0.0	53.2	0.0	11.1	4.6	0.0
SB4	CC4	0.3	0.9	77.8	29.7	0.0	4.7	9.3	0.0

[1] - SB = Soda Butte Creek, CC = Cache Creek, numbers correspond to reach number of development and test sites.

Table 17 - Percent correctly classified of each hydrogeomorphic unit in the Soda Butte and Cache Creek development and test sites as derived from producer's accuracies using the Maximum Joint Probability classification.

Hydrogeomorphic Units									
Study Sites		Eddy Drop Zone	Glide	Lateral Scour Pool	Low Gradient Riffle	High Gradient Riffle	Detached Bar	Attached Bar	Large Woody Debris
Development[1]	Test[1]								
SB1	SB1	0.0	35.2	5.9	49.6	34.4	32.2	60.7	11.2
SB1	SB4	0.0	15.9	2.7	61.0	10.4	16.5	22.0	4.1
SB1	CC2	0.0	7.8	16.8	38.9	11.5	38.8	10.8	4.4
SB1	CC4	0.0	3.8	2.5	24.3	7.9	23.2	23.8	1.7
SB4	SB4	47.7	15.2	21.1	73.7	0.0	64.6	7.9	0.0
SB4	SB1	3.9	6.5	0.3	42.9	0.0	19.3	35.8	0.0
SB4	CC2	30.0	5.4	0.0	37.8	0.0	65.3	1.6	0.0
SB4	CC4	7.3	0.9	2.0	16.0	0.0	9.6	18.6	0.0

[1] - See note at end of Table 11 describing stream reach abbreviations.

Confusion of Hydrogeomorphic Units

Eddy drop zones, high gradient riffles, and lateral scour pools were seldom correctly classified in the development sites (Tables 16 and 17). This leads to a lack of correct classification of these stream units in all test sites. Low gradient riffles and bars were most often classified correctly in the development sites leading to a higher percent correctly classified of these hydrogeomorphic units in the test sites. These classification results may be attributed, in part, to the proportion and spatial distribution of these hydrogeomorphic units in the stream channels (Table 12). Eddy drop zones, high gradient riffles, and lateral scour pools are the least frequently found units in the study site and tend to be the smallest in surface area. They are usually located adjacent to low gradient riffles and bars. Because these units are so small and infrequent, accurate classification depends heavily on precise rectification of the imagery with the raster field map. Low gradient riffles and bars comprise the majority of the study sites in terms of area and are laterally extensive in both length and width in the stream channels. Figure 7 shows the correctly classified and misclassified pixels from the Soda Butte reach 1 development site using the Maximum Joint Probability method.

To understand the results of the Maximum Joint Probability classification results, it is important to examine what the hydrogeomorphic units are most often confused (misclassifed) with. The confusion matrices of omission (Table 17, Appendix B) illustrate these results along the columns. Table 18 shows which hydrogeomorphic units are likely to be confused more than 15% of the time (rows of commission matrices, Table

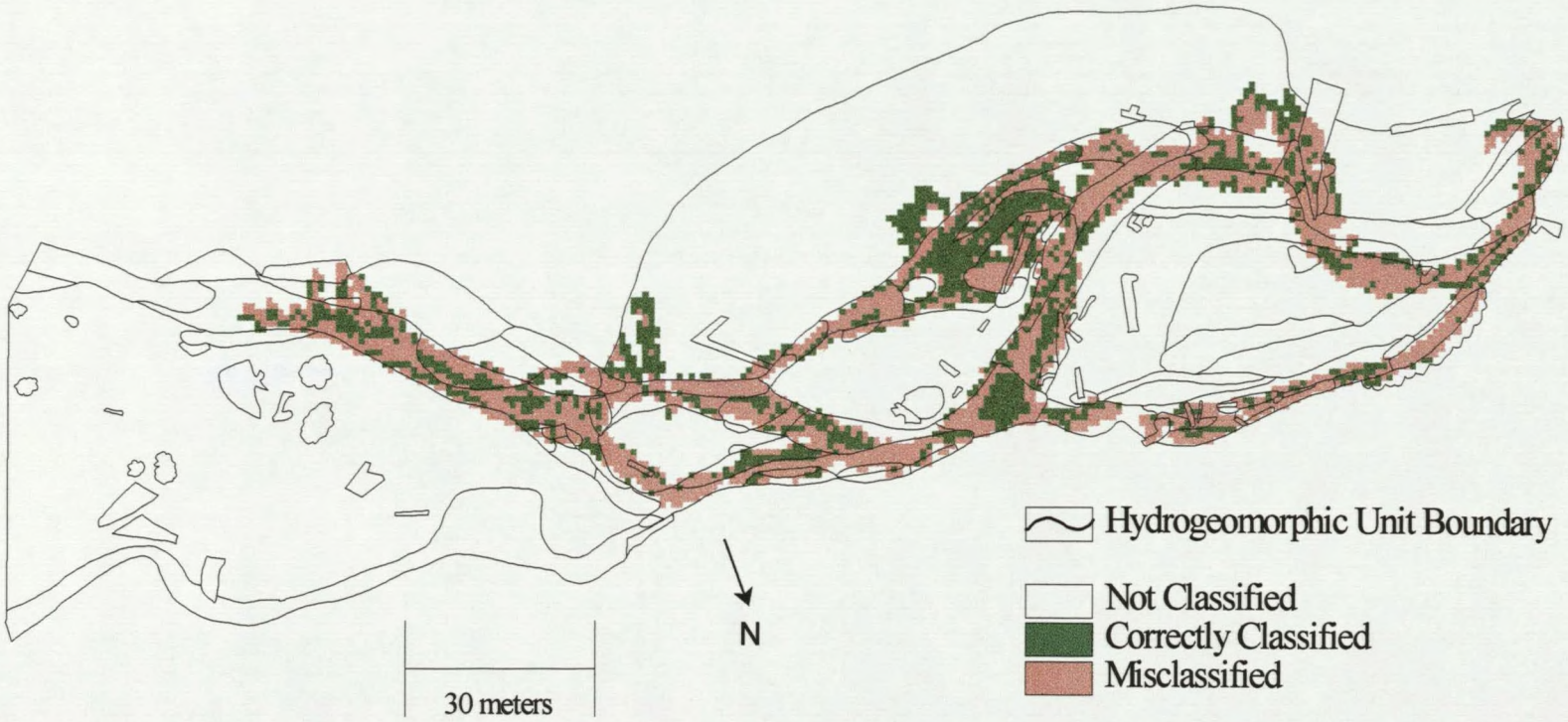

Figure 7 - Results of Maximum Joint Probability classification on Soda Butte Creek reach 1 development site showing correctly classified hydrogeomorphic units.

Table 18 - Confusion of classified hydrogeomorphic units ranked from most to least likely. Only hydrogeomorphic units confused over 15% of the time are shown in this table.

	Hydrogeomorphic Unit Most Often Confused With			
Map Class	Most			Least
Eddy Drop Zone	Low Gradient Riffle	Glide	High Gradient Riffle	Attached Bar
Glide	Low Gradient Riffle	Attached Bar	Detached Bar	High Gradient Riffle
Lateral Scour Pool	Low Gradient Riffle	Attached Bar	High Gradient Riffle	Detached Bar
Low Gradient Riffle	Attached Bar	Detached Bar	Glide	High Gradient Riffle
High Gradient Riffle	Low Gradient Riffle	Detached Bar	Attached Bar	Glide
Detached Bar	Low Gradient Riffle	Attached Bar	Glide	High Gradient Riffle
Attached Bar	Low Gradient Riffle	Glide	Detached Bar	High Gradient Riffle
Large Woody Debris	Low Gradient Riffle	Attached Bar	Glide	Detached Bar

15, Appendix B, columns of omission matrices, Table 15, Appendix B). Results are supported by both the classification developed on Soda Butte Creek reach 1 and the classification developed on Soda Butte Creek reach 4 for all test sites.

In all cases, classified hydrogeomorphic units are most often confused with the types of hydrogeomorphic unit they are adjacent to (Figs. 2 and 3). All units are confused with low gradient riffles. This is because low gradient riffles are the predominant unit in each of the study sites and cover the largest area. None of the units are confused with

large woody debris. Large woody debris is usually found on bars, not in the channels and is therefore not confused with the water units. Large woody debris also exists as a long linear feature on the map usually less than 1m wide. Given the 1m pixel size of the digital imagery, large woody debris is easily missed on the bars during the classification process. Most units are also likely to be confused with bars. Based on the hydro-geomorphic classification used in this study, bars, riffles, and glides are sedimento-logically similar, bars just lack water.

Overall, the larger the area a unit comprised, the more likely it was found to be correctly classified (e.g. low gradient riffles were correctly classified 16-74% of the time). The smaller the unit in area, the less likely it was to be classified correctly (e.g. eddy drop zones were correctly classified 0-47% of the time). In addition, hydrogeomorphic units are most often correctly classified in the center of the unit and incorrectly classified along their boundaries with other units (Fig. 7). The poor rectification and the similarity of bars and riffles from a sedimentological perspective are responsible for some of the incorrect classification of hydrogeomorphic units, especially at unit boundaries. Because bars are essentially riffles without any water, it is not surprising that they are confused with each other so often (Tables 16, 17, 18).

Problems with Rectification

Geographic reference points on Cache Creek and Soda Butte Creek were mapped on two occasions using Global Positioning Systems (GPS) but the location of study sites

in deep canyons and failures at local base stations made the location data unusable. Without this data, the imagery had to be visually rectified to the field map. The lack of precise ground control points led to poor rectification (i.e. boundary shifts of up to 2 to 5 meters) between the imagery and field maps. This made direct boundary correlation between the hydrogeomorphic units on the field map and in the imagery difficult. An example of poor rectification of the classified pixels with the field map is best shown by the misalignment of the stream channel between the imagery and the field map (Fig. 8). Geographic reference points could not be remapped at a later date because a one hundred year recurrence interval flood rearranged the channel morphology and washed away triangulation points.

Classification of the smallest hydrogeomorphic units; eddy drop zones, lateral scour pools, and high gradient riffles was most affected by the rectification problems. For these units, which are often less than $4m^2$ in area and 1 to 2 meters wide, a rectification result where the boundary is shifted by one pixel (1m) necessarily leads to a poor classification result (Hord and Brooner, 1976). Low classification accuracies in situations such as this are thus largely a function of mapping error and do not provide a good test of whether spectral reflectance provides a good mapping tool. Given this scenario, at best only 75% of that unit can be classified correctly. Larger geomorphologic units such as low gradient riffles and bars are less effected by the rectification results because a boundary shift of one meter only results in a very small percentage of that unit being necessarily misclassified. Better rectification would likely lead to the smallest units being identified more frequently and a higher percentage of the larger units being correctly classified.

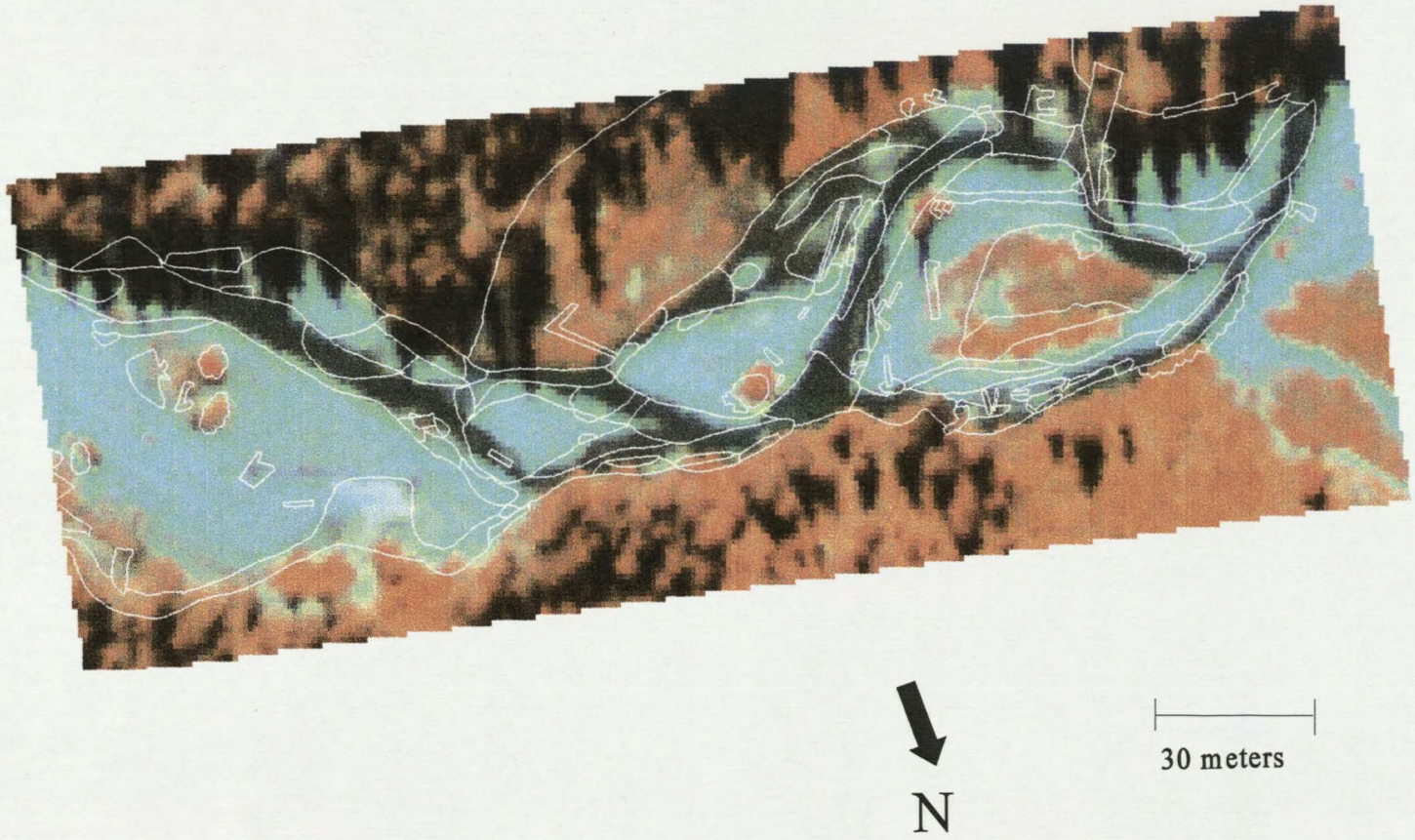

Figure 8 - Soda Butte reach 1 imagery with rectified field map of Soda Butte reach 1 overlain in white. Error in rectification of the channel between the imagery and field map is particularly visible in the upper right portion of the figure.

Sedimentology and Water Depth

Sedimentological differences between the two streams may also have effected the classification results. Cache Creek lacks the Paleozoic carbonate sediments that are present in Soda Butte Creek which may have resulted in differences in spectral reflectance between the hydrogeomorphic units in the two streams. These differences may be seen in the range of pixel values for each of the reaches (Table 11) where Cache Creek does not have the lower range of digital numbers in most bands that are present in Soda Butte Creek.

Wolman pebble counts taken on Soda Butte Creek showed that eddy drop zones were the only units that were clearly distinct in their sediment size distribution (Table 9). Eddy drop zones, however, were the least likely of all the hydrogeomorphic units to be classified correctly leading to the conclusion that sediment size was not a major factor in identifying eddys. High gradient riffles, low gradient riffles, glides, and bars had similar sediment size distributions (Table 9) which may be one explanation for why they were not effectively distinguished from one another (Table 18).

The stream channels are believed to have dropped approximately 2 to 3 cm in water level during the time between mapping and remote sensing data collection. Given the shallow nature of most of the hydrogeomorphic units in this study (Table 10), even a minor drop in water level could lead to misalignment of the boundaries of stream units on the field map and image, thus adding more difficulty to the rectification process. As more land is exposed due to a drop in water level, the hydrogeomorphic units are most effected

at their boundaries with the channel edge and bars.

Spectral Signatures

Another potential explanation for misclassification of hydrogeomorphic units is the similarity of spectral signatures developed for each type of unit. Figures 5 and 6 illustrate the mean spectral signatures developed for each hydrogeomorphic unit and the overlap of spectral signatures among units is visible. For example, the spectral signatures for glides, and high gradient riffles are contained almost entirely within the spectral signatures developed for low gradient rifffles. From a spectral perspective, therefore, these units are not distinct. This makes it extremely difficult to differentiate such hydrogeomorphic units, and these units are in fact confused with one another most often (Table 18). Shadows caused by vegetation and cloud cover may also have interfered with the development of unique spectral signatures for the hydrogeomorphic units. For example, lateral scour pools often undercut banks causing willows and trees to overhang thereby casting shadows which lead to a weak or incorrect spectral signature for these types of units.

Habitat Class Evaluation

Where the utility of the Maximum Joint Probability classification as a precise mapping tool is poor for small units, it can be used to estimate habitat classes along the mapped stream reaches. Despite the problems with rectification which cause systematic

error in classification of hydrogeomorphic units, the Maximum Joint Probability classification results can still be used to provide an estimate of the area of each reach that is comprised of the largest hydrogeomorphic units. Figure 9 compares the area of all field

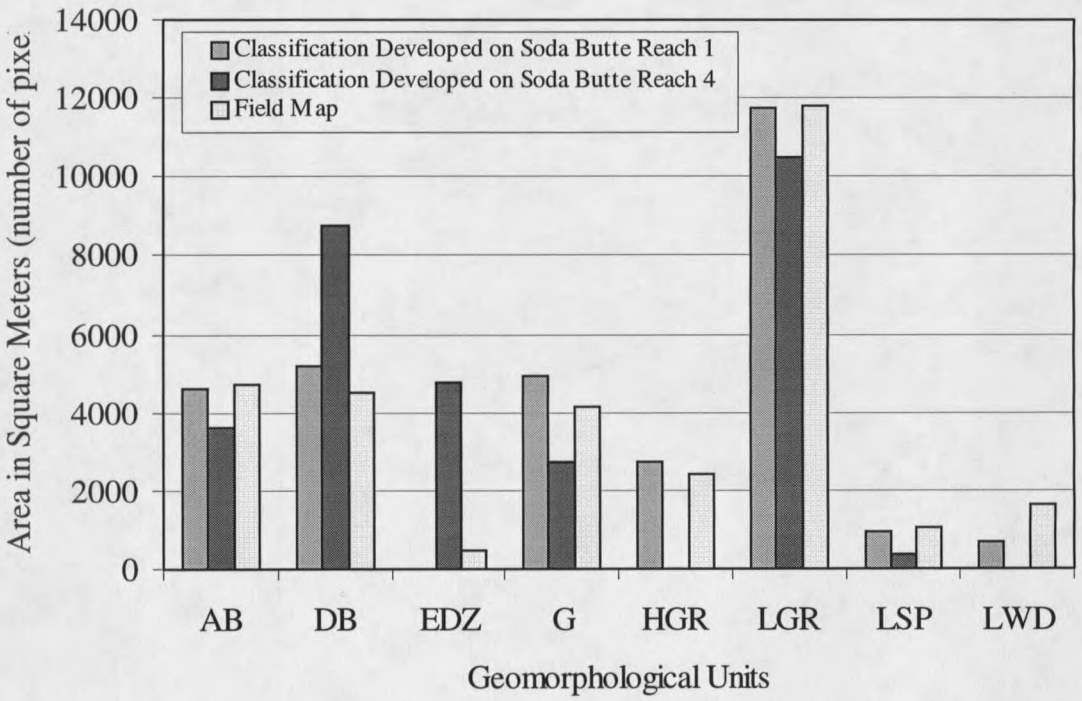

Figure 9 - Comparison of field mapped area and predicted area of hydrogeomorphic units. Area was predicted from the Maximum Joint Probability classifications developed from Soda Butte reaches 1 and 4 and tested on all stream reaches. Field mapped area is the cumulative area of all hydrogeomorphic units mapped on all four stream reaches on Soda Butte and Cache Creeks.

mapped hydrogeomorphic units to the area of all hydrogeomorphic units predicted by the Maximum Joint Probability classifications developed on Soda Butte reaches 1 and 4. The areas of low gradient riffles, high gradient riffles, glides, detached bars, and attached bars are most accurately predicted from the Maximum Joint Probability classification results. While the areas of eddy drop zones, lateral scour pools, and large woody debris are not as

well predicted, this type of analysis still gives a clear picture of how much of the reaches can be expected to be composed of these types of units. This type of analysis as a habitat evaluation tool can be useful for studies where bars and riffles are critical such as fishery habitat and heavy metal concentration studies (Ladd, et al., 1998).

ALTERNATIVE JOINT PROBABILITY CLASSIFICATION

The Maximum Joint Probability classification only allows one outcome (i.e. one classification) per image class; the one with the highest index as determined from equation 1. The Alternative Joint Probability classification relaxes the requirements for maximum joint probability by allowing each of the 30 image classes to represent more than one hydrogeomorphic unit. The seven hydrogeomorphic units are allowed to be represented by any of the image classes that have a higher probability of occurrence than random as calculated in equation 1.

The Alternative Joint Probability classification approach is especially useful for this type of study where so many of the map units are small in area and are spectrally dwarfed by the larger units (Table 11, Figures 5 and 6). For example, the map unit of eddy drop zone is never the maximum joint probability class in the Soda Butte Creek reach 1 development site classification, although it is predicted to be the second or third joint probability class in 3 of the 30 image classes. By allowing pixels in these 3 classes to be assigned to eddy drop zones as one of the lower joint probability classes, eddy drop zones are identified and overall accuracy is increased (Goodchild et al. 1992). In many

cases, the second and even third joint probability classes may be almost as likely as the Maximum Joint Probability class (e.g., the maximum joint probability class may have a joint probability index of 35 but the second and third joint probability classes may have joint probability indices of 34 and 31 respectively). This type of analysis considers a broader classification than the Maximum Joint Probability method, therefore increasing overall accuracy for the map as a whole (Aspinall and Pearson, 1995).

The total number of pixels correctly classified correctly using this method were counted and divided by the total number of pixels in the reach. The percent correctly classified using this technique (Table 19) are considerably higher than those of the Maximum Joint Probability classification (Table 13).

Table 19 - Percent correctly classified for development and test sites using all image classes with joint probabilities greater than random.

Development Site	Test Site	Percent Correctly Classified
Soda Butte Reach 1	Soda Butte Reach 1	80%
Soda Butte Reach 1	Soda Butte Reach 4	67%
Soda Butte Reach 1	Cache Creek Reach 2	59%
Soda Butte Reach 1	Cache Creek Reach 4	56%
Soda Butte Reach 4	Soda Butte Reach 4	80%
Soda Butte Reach 4	Soda Butte Reach 1	53%
Soda Butte Reach 4	Cache Creek Reach 2	55%
Soda Butte Reach 4	Cache Creek Reach 4	28%

From the Alternative Joint Probability analysis, a series of maps can be generated for each hydrogeomorphic unit in each reach tested, showing the likelihood of occurrence

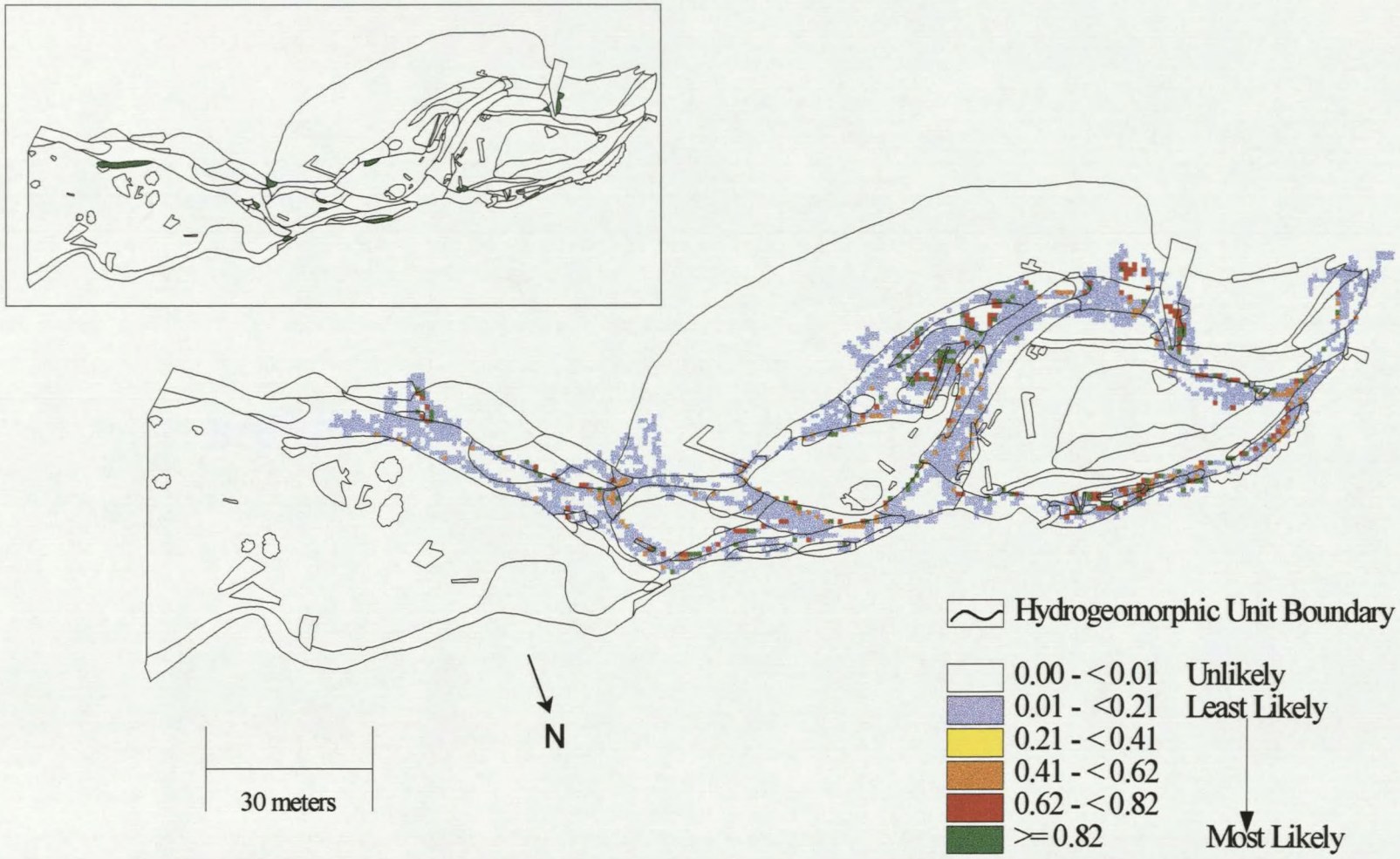

Figure 10 - Proportional results using all joint probability classes with index values greater than random for eddy drop zones. Inset shows proper location for eddy drop zones in green as mapped in the field.

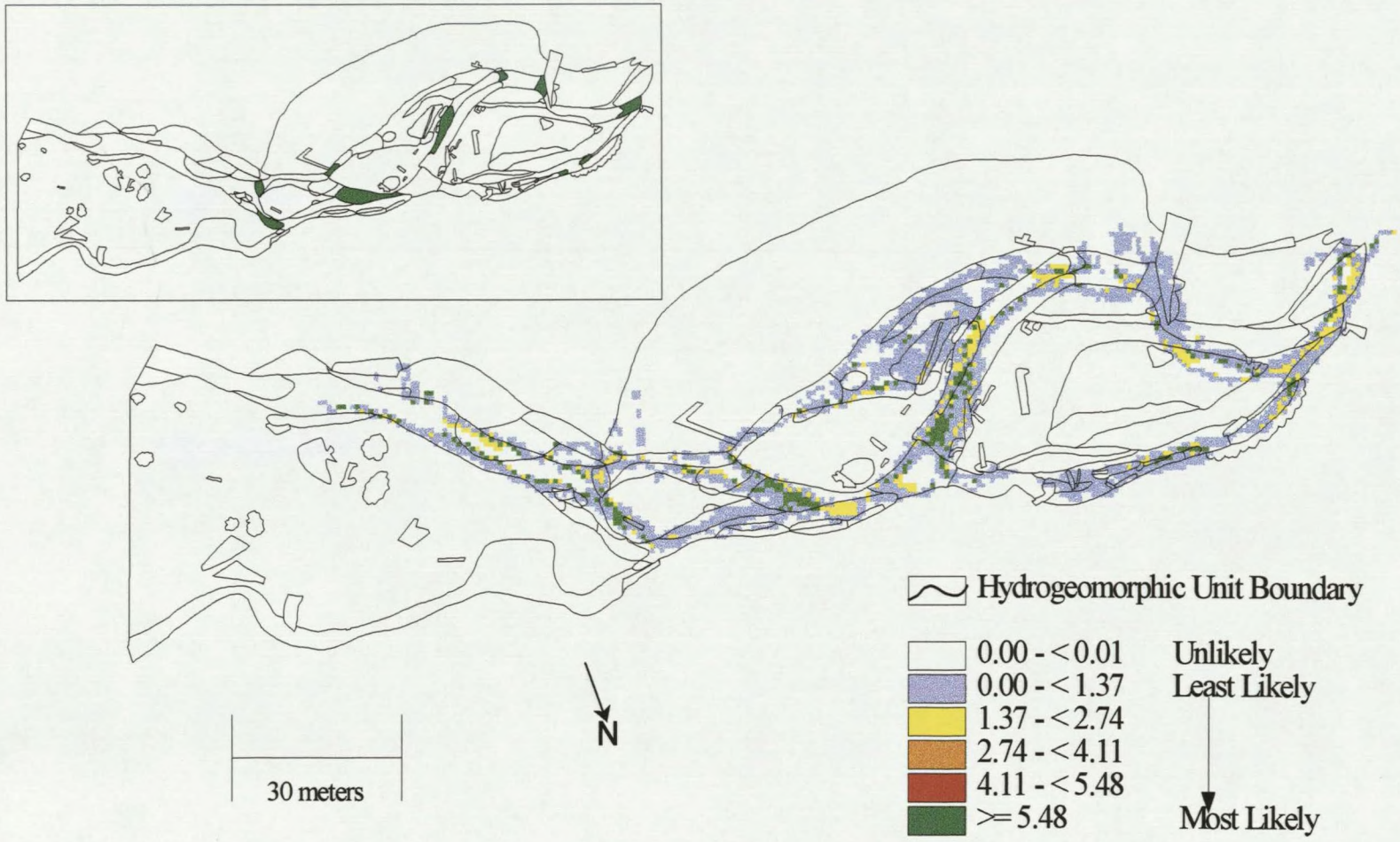

Figure 11 - Proportional results using all joint probability index values greater than random for high gradient riffles. Inset shows proper location for high gradient riffles in green as mapped in the field.